Investigating the mechanophysical and biological characteristics of therapeutic dental cement incorporating copper doped bioglass nanoparticles

■ Abstract

Objective. This study was investigated the mechanophysical properties of zinc phosphate cement (ZPC) with or without the copper doped bioglass nanoparticles (Cu-BGn) and their biological effect on dental pulp human cells and bacteria.

Materials and Methods. Cu-BGn were synthesized and characterized firstly and then, the experimental (Cu-ZPC) and control (ZPC) samples were fabricated with similar sizes and/or dimensions (diameter: 4 mm and height: 6 mm) based on the International Organization of Standards (ISO). Specifically, various concentrations of Cu-BGn were tested, and Cu-BGn concentration was optimized at 2.5 wt% based on the film thickness and overall setting time. Next, we evaluated the mechanophysical properties such as compressive strength, elastic modulus, hardness, and surface roughness. Furthermore, the biological behaviors including cell viability and odontoblastic differentiation by using dental pulp human cells as well as antibacterial properties were investigated on the Cu-ZPC. All data were analyzed statistically using SPSS® Statistics 20 (IBM®, USA). $p < 0.05$ (*) was considered significant, and 'NS' represents nonsignificant.

Results. Cu-BGn was obtained *via* a sol-gel method and added onto the ZPC for fabricating a Cu-ZPC composite and for comparison, the Cu-free-ZPC was used as a control. The film thickness (≤ 25 μm) and overall setting time (2.5~8 min.) were investigated and the mechanophysical properties showed no significance ('NS') between Cu-ZPC and bare ZPC. However, cell viability and odontoblastic differentiation, alkaline phosphate (ALP) activity and alizarin red S (ARS) staining were highly stimulated in the extracts from the Cu-ZPC group compared to the ZPC group. Additionally, the antibacterial test showed that the Cu-ZPC extracts were more effective than the ZPC extracts ($p < 0.05$).

Significance. Cu-ZPC showed adequate mechanophysical properties (compressive strength, hardness, and surface roughness) and enhanced odontoblastic differentiation as well as antibacterial properties compared to the ZPC-only group. Based on the findings, the fabricated Cu-ZPC might have the potential for use in the field of dental medicine and clinical applications.

Keywords: Dental cement, Bioactive glass, Cu-BGn, Zinc phosphate cement

1. Introduction

Dental types of cement have been widely applied in the field of restorative and orthodontic dentistry such as in cavity linings, sedative filling, temporary or permanent tooth restorations, and the joining of fixed prostheses and orthodontic band [1–6]. In particular, 'ideal' dental cement should have several characteristics: nonirritant, good resistance to dissolution in saliva and oral fluids, high mechanical strength, adequate working and setting time, and low film thickness (≤ 25 μm) for luting agent [7–10]. Cement that satisfy the aforementioned properties can be classified as zinc phosphate, polycarboxylate, zinc oxide eugenol, glass ionomer, and resin-modified glass ionomer cement [6,11–15]. Despite the advent of new cement such as glass ionomers or resin-based cement, many clinicians prefer zinc phosphate cement (ZPC) for luting cast metal prostheses because of its ease of operation, high elasticity and compressive strength, optimum coating degree, ease of excess cement removal, and cost-effectiveness [3,16,17]. Moreover, it has been indicated that the high stiffness of ZPC materials could be beneficial for reducing stresses transmitted from the restoration as a base material in the cavity [18]. However, deficiencies of ZPC include low antibacterial activity, the probability of pulp irritation due to the low pH at the beginning of hardening, no chemical adherence to teeth, and relatively high solubility in the oral cavity [3,19]. Little has been applied to overcome these limitations of ZPC, although many researchers have attempted to improve the properties of cement biomaterials by adding micro/nanoparticles as reinforcements or therapeutic fillers such as graphene oxide, and bioactive glasses [20–24].

Bioactive glasses (BGs) were first introduced in 1969 by Hench as a promising biomaterial for application in tissue regeneration [25]. A range of bioactive materials with attractive properties, such as biocompatibility and bioactivity, synthesized by novel methods have been investigated [25]. Recently, bioactive glass nanoparticles (BGn) have stood out as excellent candidates for nanostructured composites, as their small size, high surface area to volume ratio and uniformity in shape facilitate a more homogeneous distribution in comparison to their micronsized-counterparts [26–28]. The addition of BGn to other materials may exhibit synergistic effects combining osteogenic potential and satisfactory mechanical properties through the release of therapeutic metallic ions [26]. Among the variety of therapeutic ions, copper (Cu) ion-containing bioglass nanoparticles (Cu-BGn) have been proven to be able to enhance hard tissue regeneration and vascularization as well as wound healing [29–32]. Additionally, Cu-BGn is recognized to be antimicrobial, a crucial aspect for effective hard tissue repair under bacterial infection, which can be induced by the release of copper ions from the nanoparticles [33,34]. As an example, we reported that copper added to bioactive glass nanoparticles or Cu-incorporated bioactive glass nanoparticles (Cu-BGn), not only contributed to angiogenesis but also

showed antibacterial activity against *E. faecalis*, which is frequently accompanied by pulp infections [35].

Recently, Wassmann et al. used commercial Cu-modified zinc phosphate cement (Hoffmann's copper cement, Hoffmann's Dental Manufacturer, Germany) to evaluate antimicrobial activities and mechanical properties [19]. They did not find enhanced antimicrobial activities in Cu-modified zinc phosphate cement, probably due to inhomogeneity or the concentration of Cu [36,37]. To our knowledge, including the above literature, the effect of Cu-modified ZPC has rarely been investigated in terms of odontoblastic differentiation for minimizing pulp irritation. Previously, inorganic cements (e.g., strontium-releasable inorganic, calcium silicate-based, and hydroxyapatite-based cements) have been reported [38–40]. Unlike commercial Cu-modified zinc phosphate cement, inorganic dental cements have promoted odontogenic differentiation as well as shown antibacterial properties due to the released therapeutic ions.

In this study, we propose a novel Cu-doped bioglass nanoparticles (Cu-BGn) that incorporated onto the ZPC (Cu-ZPC) as a dental cement because Cu-BGn has potential to release therapeutic ions such as Cu, Ca, and Si. To obtain stable Cu-ZPC, the Cu-BGn concentration was optimized based on film thickness and net setting time. The overall characteristics of the optimized Cu-ZPC were compared with those of Cu-free-ZPC by manipulating the mechanophysical properties, such as compressive strength, hardness, and roughness, as well as the biological properties, including cell viability, odontoblastic activities, and antibacterial properties, against dental pulp human cells. The null hypothesis of this study is that there would be no significant differences in the 1) mechanophysical properties and 2) *in vitro* cellular activations between Cu-ZPC and bare ZPC.

2. Materials & Methods

2.1. Preparation of Cu-BGn and Cu-BGn-added zinc phosphate cement (Cu-ZPC)

Cu-BGn was prepared based on a previous study [41]. Briefly, 5 g of copper (Sigma–Aldrich, USA) was dissolved in 120 mL of alkaline methanol (pH = 12.5), and calcium nitrate tetrahydrate ($Ca(NO_3)_4 \cdot 4H_2O$, 99%, Sigma–Aldrich, USA) was added. In a separate batch, tetraethylorthosilicate (TEOS, 99%, Sigma–Aldrich, USA) was homogeneously dissolved in 30 mL of absolute methanol (pH = 12.5) and added to the first solution with the simultaneous application of ultrasonic homogenizers (SONOPULS). The precipitate was dried at 70 °C with a 2% molar percentage of Cu in the BGn and then replaced with a certain ratio of Ca so that the Cu:Ca:Si weight% ratio was 5:10:85. Then, 5 g of polyethylene glycol (PEG, Sigma–Aldrich, USA) was added and stirred in a sonoreactor (ULH-700S, Ulsso Hitech, Cheongju-si, South Korea) overnight. The precipitated Cu-BGn were washed three times with ethanol and then centrifuged at 5000 rpm for 5 min. After decanting the supernatant, the precipitate

was dried in an oven at 70 °C overnight, and the dried powder was finally heat-treated at 600 °C for 6 h.

As the control, commercial zinc phosphate cement (ZPC, ELITE CEMENT 100, GC, Japan) consisting of powder (88 wt% of ZnO and 12 wt% of MgO) and liquid (50 ~ 60 wt% of phosphoric acid, 3 wt% of aluminum and 37 wt% of water) was used and the cement powder mixed with Cu-BGn using a ball mill. Specifically, various concentrations of Cu-BGn were tested, and the optimized Cu-BGn concentration was set at 2.5 wt% based on the film thickness and overall setting time, which was referred to as Cu-BGn-incorporated zinc phosphate cement (Cu-ZPC). Next, we evaluated mechanophysical properties such as compressive strength, hardness, and surface roughness. Here, the control and Cu-ZPC were formed by manual mixing in a liquid/powder ratio of 0.5 mL/1.45 g, according to the manufacturer's instructions.

2.2. Characterization of Cu-ZPC

Optical microscopy and field emission scanning electron microscopy (FE-SEM, Sigma 300, Zeiss, Germany) were used to observe the surface morphologies. Additionally, the energy-dispersive spectroscopy (EDS; UltraDry, ThermoFisher, Waltham, MA, USA) was conducted to determine the distribution of the copper, calcium, and silicon particles in the ZPC. To analyze the phase of the sample, X-ray diffraction (XRD, Ultima IV, Rigaku, Japan) was used in the range of 20° ~ 80° by the theta/2theta method. Cu Kα radiation at 40 mA and 40 kV, with a step size of 0.02° and a scanning rate of 2°/min. was used.

The film thickness was measured in accordance with the annex of ISO 9917-1:2007. The initial thickness of two glass plates (200 mm × 25 mm × 5 mm) was precisely measured using an electronic caliper with an error range of 1 μm. Thereafter, 0.10 ± 0.05 mL of cement was mixed and placed in the center between the glass plates, and a load of 150 N was applied for 15 min (n = 5). The net setting time was measured at 37 °C and 100% humidity using an indenter of mass (400 ± 5 g) with the flat end of the needle having a diameter of 1 ± 0.1 mm. Each sample was loaded with the needle, and the appearance of the needle imprint was observed to determine the setting time (n = 3).

The mechanical strength was measured in accordance with the annex of ISO 9917-1:2007. The cement was injected into a cylindrical metal mold with a diameter of 4.0 ± 0.1 mm and a height of 6.0 ± 0.1 mm, stored for 1 h in a cabinet at 37 ± 1 °C and 50% relative humidity. Then, the sample was embedded in distilled water at 37 °C for 24 h. A material tester (Instron 5596, Norwood, MA, USA) was set at a rate of 1 mm/min before the strength at the fracture was measured and set as p. Then, the compressive strength (C) was calculated according to the following formula (n = 10):

$$\mathrm{C} = \frac{4p}{\pi d^2}\ (\mathrm{MPa})$$

where p is the maximum load applied at the fracture (N), and d is the specimen diameter (mm). The compressive modulus (elastic modulus) was determined from the linear slope of the stress-strain curve during the compression test of samples.

The surface roughness (R_a and R_z) was automatically measured in 4 places per specimen using a surface roughness measuring device (SJ-400, Mitutoyo, Japan) with the stylus method (n = 4). Among the hardness test methods suitable for characterizing dental cement, the micro-Vickers hardness (HM-221, Mitutoyo, Japan) test method was used. A load of 200 gf was applied for 20 s, and the Vickers hardness (HV) was calculated according to the following formula (n = 7):

$$\mathrm{HV} = 1.8544 \frac{\mathrm{P}}{d^2} (\mathrm{kgf/mm^2})$$

where HV is the hardness Vickers, P is the load (kgf), and d is the mean diagonal length of indentation (mm).

2.3. In vitro cytotoxicity test of Cu-ZPC

Dental pulp human cells were isolated from the vital primary teeth of healthy children (aged 5 years old, male, without any systemic disease and with caries-free teeth) after written consent was obtained from their guardians. The primary mandibular incisor was extracted due to the abnormal eruption of the permanent successor, and all procedures were approved by the Ethical Committee of the Institutional Review Board of Dankook University Dental Hospital (IRB number DKUDH 2019-10-001). The minced pulp tissue was added to the phosphate-buffered solution (PBS; Gibco, Grand Island, NY, USA) supplemented with 1% penicillin/streptomycin (Gibco). After incubation for 1 h at 37 °C with 2 mg/mL collagenase type I (Worthington Biochemical, Lakewood, NJ, USA) and 4 mg/mL dispase II (Invitrogen, Carlsbad, CA, USA), the solution was centrifuged at 1500 rpm for 3 min. The cells were cultured in α-MEM with 10 % FBS, 1 % penicillin/streptomycin, 2 mM GlutaMAX, and 1 mM L-ascorbic acid and incubated in a humidified atmosphere containing 5% CO_2 at 37 °C. Cultured dental pulp human cells (cell density: 1×10^5 cells/mL) at passage 5 were used for the experiments, and the medium was changed every 2 days.

The extracted groups were obtained to test for cytotoxicity, odontoblastic differentiation, and antibacterial properties. For use in the cytotoxicity and odontoblastic differentiation, α-MEM modification solution (Gibco) was prepared with the addition of 10% FBS, 1% penicillin/streptomycin, 2 mM GlutaMAX, and 1 mM L-ascorbic acid. For the antibacterial experiments, α-MEM modification solution (HyClone Laboratories Inc., USA) containing L-glutamine, ribonucleosides, and deoxyribonucleosides was prepared. The 100% extracts of the ZPC and Cu-ZPC specimens (size: 15 mm of diameter and 1 mm of height and extraction ratio (surface area or mass/volume; 1 mm of

thickness): 3 cm^2/mL) based on the ISO requirement (ISO-10993) were added to 1.34 mL of α-MEM modification solution composed of the addition of 10% FBS, 1% penicillin/streptomycin, 2 mM GlutaMAX, and 1 mM L-ascorbic acid for cytotoxicity and odontoblastic differentiation and 1.34 mL of α-MEM modification solution containing L-glutamine, ribonucleosides, and deoxyribonucleosides for the antibacterial test, treated in a shaking incubator for 24 h, and filtered through a 0.2 μm size filter. The obtained extract was repeatedly diluted by half to make the extracts of various concentrations required for the experiments. The elemental releases (ppm; mg/L) of Zn, Cu, Ca, and Si was determined *via* inductively coupled plasma atomic emission spectroscopy (ICP-AES, OPTIMA 800, Perkin-Elmer, USA) (n = 3) [39]. To observe the acid and/or base levels of the extracted ZPC and Cu-ZPC, the pH of the original and diluted extracts with α-MEM were measured using a digital pH meter (Orion 4 Star, Thermo Scientific Pierce, IL, USA) (n = 3).

Cell viability was assessed according to ISO 10093-5:2009. Dental pulp human cells were placed in a 96-well plate with 100 μL of the medium, incubated for 24 h, and then washed with PBS. Then, different extract concentrations (0~100%) were added to ZPC and Cu-ZPC and incubated for 24 h based on the MTS assay (CellTiter 96 Aqueous One Solution Cell Proliferation Assay, Promega, Madison, WI, USA). As the controls, negative (dental pulp human cells cultured in growth medium) and positive (dental pulp human cells cultured in differentiation medium) controls were used. The optical density (OD) was measured by a microplate reader (SpectraMax M2e, Molecular Devices, Sunnyvale, CA, USA) at a wavelength of 490 nm (n = 5). A live/dead assay was conducted by staining samples with 0.15 mM calcein AM and 2 mM ethidium homodimer-1 for 45 min to evaluate cell viability. The fluorescently stained live (green) and dead (red) cells were visualized under a confocal laser scanning microscope (CLSM, LSM700, Carl Zeiss, Thornwood, NY, USA).

To determine the odontoblastic differentiation of the dental pulp human cells, noncytotoxic diluted extracts of 25% and 12.5% were added and cultured, followed by alkaline phosphatase (ALP) activity assay and alizarin red S (ARS) staining. ALP activity was determined on Day 7. The cells, diluted extracts of 25% and 12.5%, were washed two times with PBS (pH = 7.0) and then incubated in 10 mM Tris buffer (pH = 7.5) containing 0.1% Triton X-100 for 10 min. Then, 100 mL of lysate was added to a 96-well plate containing 100 mL *p*NPP solution. On Day 14, the cells were stained with Alizarin red S (pH = 4.2). The cells were washed three times with PBS and fixed with 70% (v/v) bioethanol at 4 °C for 1 h. Then, the ethanol-fixed cells were stained with 2% Alizarin red S reagent for 30 min. After staining and washing five times with distilled water, optical images of the ALP activity and ARS staining were taken *via* light microscopy (Olympus IX71, Shinjuku, Tokyo, Japan). All analysis were performed in triplicate.

2.4. In vitro antibacterial test of Cu-ZPC

E. faecalis (ATCC 19433) was purchased from the American Type Culture Collection (ATCC; Manassas, VA, USA). All bacterial extracts, which had been kept in glycerol stock solution in a – 80 °C deep freezer, were streaked on plates of tryptic soy agar (TSA, Difco Laboratories, Becton Dickinson, Sparks, MD, USA) and incubated at 35 ± 2 °C for 18 h. A single colony of *E. faecalis*, after incubation, was transferred to a tryptic soy broth medium (TSB, Difco Laboratories, Sparks, MD, USA) and incubated while shaking. All bacterial extracts were routinely grown in their culture medium for 1 h under aerobic conditions at 35 ± 2 °C for 18 h to produce 1×10^9 CFU (colony forming unit)/mL. After 18 h incubation, we diluted *E. faecalis* from 1×10^9 CFU/mL to 2×10^6 CFU/mL. Then, the diluted extracts of various concentrations (6.25~100%) were prepared (100 μL) and mixed with 100 μL of *E. faecalis* (2×10^6 CFU/mL). Next, the bacteria-extract mixtures were treated in a shaking incubator for various treatment times (1~3 h). Finally, 20 μL of PrestoBlue was added. The extracts were observed under a light microscope, and the optical density (OD) was measured at 570~600 nm at 30 min intervals using a microplate reader (BioTek, Winooski, USA) (n = 8). The plate counting method was performed in an agar medium to observe the live bacteria more accurately. Additionally, the composite solution (100 μL of the extracts of various concentrations (6.25~100%) and 100 μL of 2×10^6 CFU/mL of *E. faecalis* without adding ZPC and Cu-ZPC extracts) was used as a control for investigating the antibacterial effect of ZPC and Cu-ZPC extracts. All analysis were performed in triplicate and we added the representative data and image.

2.5. Statistical analysis

The data are presented as the means ± standard deviation (SD), and the comparisons were analyzed statistically using SPSS® Statistics 20 (IBM®, USA). $p < 0.05$ (*) was considered significant, and 'NS' represents nonsignificant. All analysis were performed at least three times and we added the representative data and image in this manuscript.

3. Results

The fabrication of copper bioglass nanoparticles (Cu-BGn) *via* a sol-gel method is represented schematically in the **Fig. 1A**. Following condensation, gelation, and drying, a homogeneous Cu-BGn powder was obtained. The morphology and crystal structure of Cu-BGn powder was characterized by FE-SEM imaging and X-ray diffraction (XRD) (**Fig. 1B, C**). Additionally, the representative EDS spectra showed a chemical composition of 9.28 ± 0.4% Cu, 5.89 ± 0.8% Ca, and 84.83 ± 0.4% Si (wt%)

(**Fig. 1D**).

Schematic, optical, and SEM images of the fabricated ZPC and Cu-ZPC (Cu-BGn incorporated ZPC) are shown in **Fig. 2A**. Here, we fabricated cylindrical films with similar volumes and/or dimensions (10 mm × 10 mm × 2 mm) to evaluate the characteristics of ZPC and Cu-ZPC. The Cu-BGn nanoparticles were well distributed on the ZPC surface. The film thickness of each specimen was measured for different additions of Cu-BGn (1.5~3.5 wt%), as illustrated in **Fig. 2C**. When the Cu-BGn concentration was increased, the film thickness gradually increased (ZPC (control): 21 ± 3.5 μm, Cu-ZPC-1.5: 18 ± 2 μm, Cu-ZPC-2.5: 21 ± 3.5 μm, and Cu-ZPC-3.5: 36 ± 7.9 μm). Considering the ISO requirements (film thickness ≤ 25 μm), we selected ZPC as the control and Cu-ZPC-2.5 (Cu-ZPC) as the experimental group. **Fig. 2B** shows the XRD analysis and the result showed that ZnO peaks for Cu-ZPC were the same as that of the control (ZPC), and there was no significance between ZPC and each group in terms of setting time (**Fig. 2B**). The net setting time of Cu-ZPC (7.00 ± 0.3 min) was slightly decreased from the unmodified control cement (7.88 ± 0.3 min), which was within the required requirement range (2.5~8.0 min) specified in ISO 9917-1.

Compressive tests showed no significant difference between ZPC (compressive strength: 120 ± 12 MPa and elastic modulus: 6.15 ± 0.85 GPa) and Cu-ZPC (compressive strength: 105 ± 9 MPa and elastic modulus: 6.20 ± 0.46 GPa) as shown in **Fig. 2D and E**. Vickers hardness revealed no significant differences between ZPC (42.1 ± 1.7 kgf/mm^2) and Cu-ZPC (41.4 ± 1.8 kgf/mm^2) (**Fig. 2F**). Additionally, the values of the arithmetic mean of the roughness (R_a = 0.53 ± 0.01 μm for ZPC and 0.55 ± 0.04 μm for Cu-ZPC), and the ten-point average roughness (R_z = 3.1 ± 0.05 μm for ZPC and 2.8 ± 0.2 μm for Cu-ZPC) were investigated (**Fig. 2G**). All surface roughness aspects (R_a and R_z) showed similar trends among the groups.

The extracts from each group were obtained for use in the cytotoxicity, odontoblastic differentiation, and antibacterial experiments. For elemental analysis, the released Zn, Cu, Ca and Si ions in the 100% extract were analyzed for ZPC (Zn: 24.77 ± 0.15 ppm, Cu: Not detected, Ca: 12.31 ± 0.06 ppm, Si: Not detected) and Cu-ZPC (Zn: 27.68 ± 0.11 ppm, Cu: 2.33 ± 0.01 ppm, Ca: 39.33 ± 0.43 ppm, Si: 10.64 ± 0.09 ppm) (**Fig. 3A**). Also, the pH measurements in different extract concentration in culture media (12.5~100%) for ZPC (12.5%: 7.92 ± 0.03, 25%: 7.97 ± 0.01, 50%: 7.93 ± 0.02, 100%: 7.77 ± 0.03) and Cu-ZPC (12.5%: 8.27 ± 0.06, 25%: 8.43 ± 0.02, 50%: 8.51 ± 0.01, 100%: 8.47 ± 0.01) were investigated. From the results, Cu-ZPC extracts showed higher trends compared to the bare ZPC extracts (**Fig. 3B**).

Cell viability test was conducted by the MTS assay and a day after seeding cells, supernatant of ZPC and Cu-ZPC specimens were treated (%) (**Fig. 4A**). The representative images for live/dead staining revealed comparable dental pulp human cell viability results only in the case of 50% extract

culture media (**Fig. 4B**). In the case of 100% extract concentration, both ZPC and Cu-ZPC showed low cell viability, but in the case of 50%, the cell viability was significantly higher in only Cu-ZPC. Next, odontoblastic differentiation studies (ALP activity and ARS staining) were performed by using dental pulp human cells. From the differentiation results on different extract concentrations of ZPC and Cu-ZPC, the optical image of the Cu-ZPC cultured on 25% extract culture media revealed a darkened color concerning ALP activity on Day 7 as well as ARS staining on Day 14 (**Fig. 5A, B**).

The antibacterial test was conducted on the control (100 μL of the extracts of various concentrations (6.25~100%) and 100 μL of 2×10^6 CFU/mL of *E. faecalis* without adding ZPC and Cu-ZPC extracts) and different ZPC and Cu-ZPC extract concentrations (6.25~100%). Optical images of the different extract plates for visualizing the living bacteria on the control (medium only; 28×10^3 CFU/mL) and ZPC 100% (29×10^3 CFU/mL) and Cu-ZPC 100% (21×10^3 CFU/mL) extracts are shown in **Fig. 6A**. Additionally, the bacterial results on the Cu-ZPC extract concentrations (6.25~100%) and the extract treatment times (1~3 h) in the culture medium were relatively lower than those of the control or extracts of ZPC (6.25~100%) (**Fig. 6B-D**).

4. Discussion

Our hypothesis is that there are no significant differences in the 1) mechanophysical properties and 2) *in vitro* cellular activations among each group because of the low amounts of additives (2.5 wt% Cu-BGn) in ZPC. The mechanophysical properties (e.g., compressive strength, compressive modulus, surface roughness, and hardness tests) had no significance among the groups, and the first null hypothesis was approved. Unlike the mechanophysical properties, *in vitro* tests (e.g., cell viability, odontoblastic differentiation, and antibacterial effects) demonstrated that the Cu-ZPC showed enhanced biological properties than the ZPC group by using different extracts. Therefore, the second hypothesis was rejected. This result can be explained by the distribution of Cu-BGn in the ZPC enhanced dental pulp human cell differentiation as well as antibacterial effects [35].

Firstly, we examined morphology and chemical compositions of Cu-BGn (**Fig. 1**). The XRD result (**Fig. 1C**) confirmed the amorphous structure of Cu-BGn, as evidenced by the complete absence of XRD diffraction peaks and the presence of a broad halo (at $2\Theta = 20° \sim 30°$) [35]. Additionally, the Cu-BGn powder had an elemental composition of Cu:Ca:Si = 9.28 ± 0.4:5.89 ± 0.8:84.83 ± 0.4 (weight % ratio). As seen in the analysis and mapping images, the weight fractions of the Cu-BGn specimen were almost similar to that of the ideal designed weight % ratio of Cu-BGn (Cu:Ca:Si = 10:5:85) (n = 3) (**Fig. 1D**) [34]. Summarizing, it can be expected that BGn and BGn-derivates could significantly affect to the cellular activities as well as surface characteristics [42,43].

Next, Cu-BGn were mixed on ZPC for fabricating a Cu-ZPC composite and its mechanophysical properties were analyzed. As shown in SEM images in **Fig. 2A**, Cu-BGn was distributed with Cu-ZPC, whereas Cu-BGn was not formed with Cu-free-ZPC. Additionally, the XRD results demonstrate that the ZnO composition on Cu-ZPC was the same as that of the control (ZPC) (**Fig. 2B**). These trends indicate that Cu-ZPC cannot affect the typical crystallinity on ZPC [44]. The film thickness is the primary consideration in luting cement which is mainly affected by the particle size, liquid/powder ratio, viscosity, and temperature [9,10]. It is measured by the minimum thickness of the cement when it is hardened under constant load conditions. As shown in **Fig. 2C**, the film thickness was gradually increased as the concentration of Cu-BGn increased. In particular, the thickness of 3.5 wt% Cu-BGn incorporated ZPC (36 ± 7.9 μm) was found to exceed the range of ISO 9917-1 (film thickness ≤ 25 μm). Based on the ISO requirement, we selected ZPC (22 ± 1.7 μm) as the control and Cu-ZPC-2.5 (2.5 wt% Cu-BGn incorporated in ZPC; 21 ± 3.5 μm) as the experimental group and named Cu-ZPC (n = 5). Regarding the hardening time of cement, various terms and measurement methods have been suggested by many researchers [45–47]. In this study, according to the definition of ISO 9917-1, the “net setting time” was "the time measured from the end of mixing, until the material has set according to the criteria and conditions". There was no significant difference in the net setting time between ZPC (7.88 ± 0.3 min) and Cu-ZPC (7.00 ± 0.3 min), and the range of net setting times is satisfactory based on the ISO requirements (2.5~8 min) ($p > 0.05$).

The mechanical properties of biomaterials represent the intrinsic properties that directly respond to external forces [48]. When considering that dental cement is mainly placed in the harsh environment of the posterior teeth, these external forces are the mastication pressure of hundreds of Newtons or the continuous abrasion caused by repeated bruxism [49,50]. Compressive strength is a property that resists the most typical force received by cement, that is, the masticatory force [48]. When measured according to the ISO standard test method, there was no significant difference between ZPC (compressive strength: 120 ± 12 MPa and compressive modulus: 6.15 ± 0.85 GPa) and Cu-ZPC (compressive strength: 105 ± 9 MPa and compressive modulus: 6.20 ± 0.46 GPa), and both satisfied the ISO requirements (≥ 50 MPa) (**Fig. 2D, E**) (n = 10). Hardness in dental cement is largely represented by abrasion resistance [48]. Abrasion is determined not only by hardness but also by many factors, such as the microstructure of the surface to be contacted, temperature, and friction [50,51]. However, in many cases, hardness and abrasion resistance show a correlation [52]. As mentioned above, high abrasion resistance is not necessarily a good feature, so determining the optimal range is important. In **Fig. 2F**, a micro-Vickers hardness test method was selected for measuring the hardness of luting cement with high brittleness and small thickness. From the data, there was no significant difference between ZPC and Cu-ZPC ($p > 0.05$). With respect to dental prostheses, surface roughness is mainly discussed as a major factor associated with mechanical stability and/or rocking. Previous studies reported that the biofilm formation

and/or retention increased as the surface roughness of luting cement and/or prosthesis increased [53,54]. **Fig. 2G** shows the arithmetic mean roughness (R_a = ZPC: 0.53 ± 0.01 μm for ZPC and 0.55 ± 0.04 μm for Cu-ZPC) and the ten-point average roughness (R_z = 3.1 ± 0.05 μm for ZPC and 2.8 ± 0.2 μm for Cu-ZPC). Based on the surface roughness results, there were no significant differences between the control and experimental groups ($p > 0.05$). These mechanophysical results attributed that the fabricated Cu-ZPC seems stable as a luting cement.

Before performing biological assays, the different elemental ion compositions (Zn, Cu, Ca and Si ions) were investigated in extracts of ZPC (Zn: 24.77 ± 0.15 ppm, Cu: Not detected, Ca: 12.31 ± 0.06 ppm, Si: Not detected) and Cu-ZPC (Zn: 27.68 ± 0.11 ppm, Cu: 2.33 ± 0.01 ppm, Ca: 39.33 ± 0.43 ppm, Si: 10.64 ± 0.09 ppm) (**Fig. 3A**). As expected, Cu and Si were presented only in Cu-ZPC, and the percentages of Ca were also relatively higher in Cu-ZPC owing to the Cu-BGn distribution and their compositions (Cu, Ca, and Si) (n = 3) [55,56]. From the ion composition results, cell viability, odontoblastic differentiation, and antibacterial properties were evaluated by using different extract concentrations of ZPC with/without Cu-BGn. **Fig. 3B** shows the pH results in different extract concentration in culture media (12.5~100%) for ZPC (12.5%: 7.92 ± 0.03, 25%: 7.97 ± 0.01, 50%: 7.93 ± 0.02, 100%: 7.77 ± 0.03) and Cu-ZPC (12.5%: 8.27 ± 0.06, 25%: 8.43 ± 0.02, 50%: 8.51 ± 0.01, 100%: 8.47 ± 0.01). From the measurement results, Cu-ZPC extracts showed a slightly higher pH tendency compared to the ZPC extracts owing to the high concentrations of therapeutic ions as well as the OH^- ion concentrations of hydrolysis by BGn (n = 3) [57,58].

Cell viability is a significant factor because it directly affects to proliferation and differentiation [59]. To observe cell viability, dental pulp human cells were stained with calcein-AM (live cells) and ethidium homodimer-1 (dead cells). **Fig. 4A and B** showed the relative cell viability results for different extracts of various concentrations by MTS assay, including the fluorescence images of live (green) and dead (red) cells. At 100% extract concentration in culture media, both ZPC and Cu-ZPC showed low cell viability (< 20%), probably owing to the alkaline pH and high extract ion concentrations confirmed by previous data [57]. However, at a 50% extract concentration in culture media, the cell viability was significantly higher in Cu-ZPC (92.8 ± 3.47%) than in ZPC (17.48 ± 0.64%) (n = 5). This can be explained because the released therapeutic ions in the Cu-ZPC extracts (Cu: 2.33 ± 0.01 ppm, Ca: 39.33 ± 0.43 ppm, Si: 10.64 ± 0.09 ppm) are much higher than that of ZPC (Cu: Not detected, Ca: 12.31 ± 0.06 ppm, Si: Not detected) based on element analysis [34,35,57]. It has been well known that the release of Cu ion results in a higher degree of cytotoxicity [60,61]. Unlike the conventional knowledge, however, our results display the opposite: the experimental group with higher cell viability. The reason for this phenomenon was not clear but there are contradictory findings of the cell viability of Cu-BGn. Wu et al. reported a decrease in cell number when hMSCs were exposed toward increasing concentrations of Cu-BGn whereas no cytotoxic effects were observed [31]. Recently, Westhauser et al.

suggested that cell viability of MSCs increased with increasing concentration of Cu-BGn [62]. Combined with 50% extract result and previous literature, Cu-BGn might be sufficiently contributing to the neutralization of cytotoxicity as an additive to cement. Next, the odontoblastic differentiation was conducted by setting the range to 0~25% extract in both alkaline phosphate (ALP) activity and alizarin red S (ARS) staining because above 50% extract had an effect on cytotoxicity. In particular, ALP is an early marker of dental pulp human cell differentiation, and the optical images showed a highly darkened violet color in the Cu-ZPC 25% extract cell culture for Day 7 (**Fig. 5A**). Furthermore, the calcium deposition in the dental pulp human cells cultured for 14 days was visualized by ARS staining to qualitatively compare mineralization in each group (**Fig. 5B**). The red color indicates that the calcium was significantly denser in the Cu-ZPC 25% extract, indicating much greater mineralization. These results might be due to the presence of therapeutic ions (e.g., Cu and Si ions) released within the Cu-ZPC 25% extract, stimulating odontoblastic differentiation [34,35,57]. Therefore, dental pulp human cells differentiated into odontoblast-like cells in the Cu-ZPC 25% extract.

Previously, ZPC showed high antibacterial activity, almost comparable to that of penicillin, immediately after mixing [63,64]. In this study, extracts from the cement were eluted using a solution reproducing the wet environment in the oral cavity, and the set antibacterial activity was evaluated with the extract. **Fig. 6A** represents the optical images of different extract plates for visualizing the living bacteria, and the counting method was performed to check the number of living bacteria on the control (medium only; 28×10^3 CFU/mL) and the ZPC 100% (29×10^3 CFU/mL) and Cu-ZPC 100% (21×10^3 CFU/mL) extracts. All analysis were performed in triplicate and the representative data and image were added in **Fig. 6A**. When the bacteria-extract mixture (100 μL of the extracts of various concentrations (6.25~100%) and 100 μL of 2×10^6 CFU/mL of *E. faecalis* without adding ZPC and Cu-ZPC extracts) was irradiated at a specific wavelength for measuring the antibacterial effect based on the Presto Blue, the absorbance increased as the number of bacteria increased. Based on the CFU measurement result, the bacterial number was dramatically reduced in Cu-ZPC 100% due to the Cu-BGn distribution. **Fig. 6B-D** shows the optical density result of different extracts (6.25~100%) of ZPC and Cu-ZPC up to different extract treatment times (1~3 h). As expected, the results from the Cu-ZPC extracts (6.25~100%) were relatively lower than those from the control (0% extract) or the ZPC extracts (6.25~100%). This can be explained by the more presence of therapeutic ion concentrations within the Cu-ZPC extracts, which is directly related to a reduction in bacterial viability [41,65,66]. Based on the results, ZPC did not show antibacterial activity as in the previous study, whereas Cu-ZPC showed significant set activity in both experiments. It seems that ZPC with copper is an interesting set combination, while Cu-BGn might be neutralized cytotoxicity to affect dental pulp human cells. Therefore, the fabricated Cu-ZPC is expected to reduce secondary caries, which leads improved prognosis of dental tissue regeneration.

5. Conclusion

In this study, we fabricated Cu-ZPC consisting of 2.5 wt% Cu-BGn incorporated into ZPC. By manipulating the mechanophysical characteristics by adjusting the Cu-BGn concentration, the film thickness, net setting time, compressive strength, compressive modulus, hardness, and surface roughness were optimized according to the International Organization of Standards (ISO). For applications in odontoblastic activations, biological activations (e.g., cell viability, ALP activity, ARS staining, and antibacterial activity) were studied, and the Cu-ZPC extract showed significant results compared with the control (ZPC extract). Therefore, Cu-BGn incorporated dental cement (Cu-ZPC) plays a promising role in dental tissue regeneration as well as in biomedical engineering field. To elaborate on this study, the use of more diverse cement will be needed in the future, while efficacy and stability evaluations through animal experiments are believed to be required for clinical application.

Acknowledgments: This work was supported by a National Research Foundation of Korea (NRF) grant funded by the Global Research Development Center Program (2018K1A4A3A01064257), by the medical research center program (2021R1A5A2022318), by the Ministry of Science and ICT (2019R1C1C1002490, 2020R1A2C1005867) and by the Priority Research Center Program provided by the Ministry of Education (2019R1A6A1A11034536). Additionally, this work was supported by a National Research Foundation of Korea (NRF) grant funded by the Korean government (MSIT) (2021R1C1C1010005) and was also supported by the research fund of Dankook University for the 2019 university innovation support program.

Conflicts of Interest: The authors declare no conflicts of interest.

▪ **Figures**

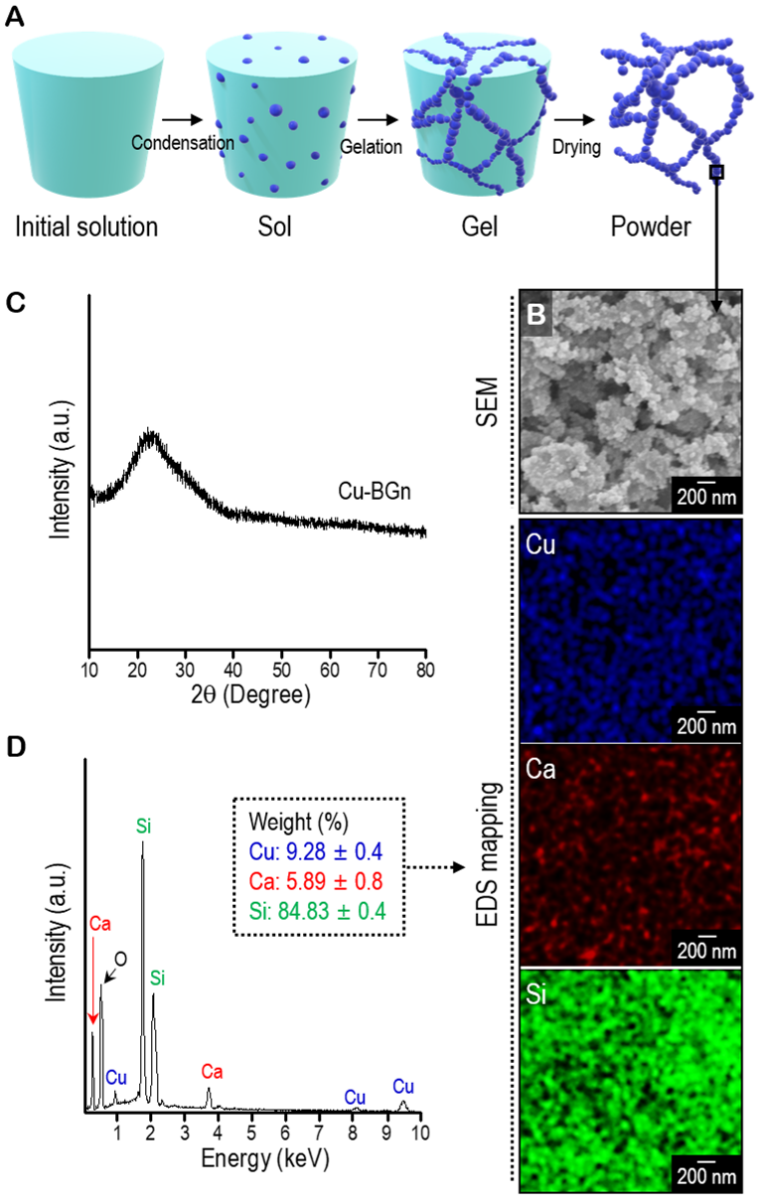

Fig. 1. Characterization of the copper bioglass nanoparticles (Cu-BGn). (A) Schematic illustration of the fabrication of the copper bioglass nanoparticles (Cu-BGn) *via* a sol-gel method including the (B) SEM image. (C) XRD spectra confirming the amorphous formation and (D) EDS result confirming that Cu-BGn has values almost identical to the ideal designed weight % ratio of Cu-BGn (Cu: Ca: Si = 10: 5:85) (n = 3).

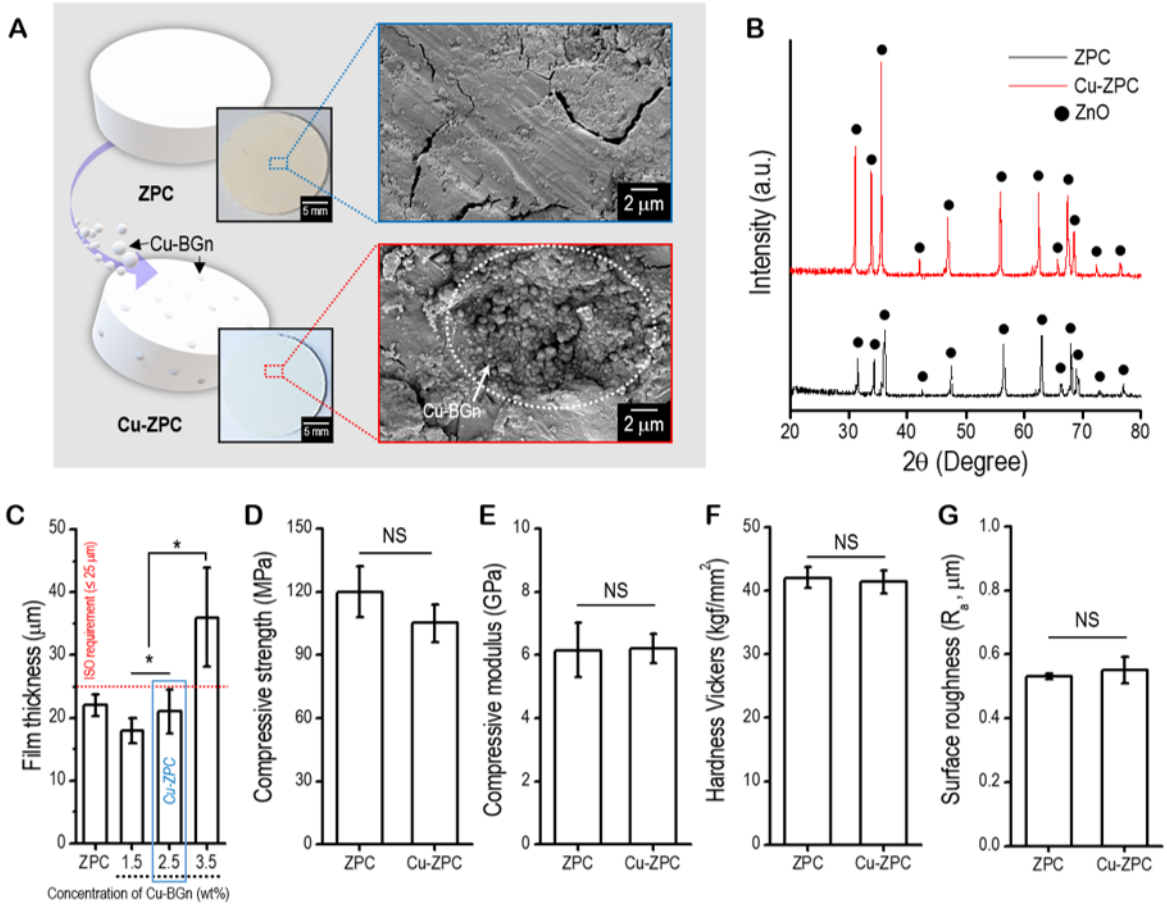

Fig. 2. Mechanophysical properties of the Cu-BGn incorporated ZPC. (A) Schematic, optical, and SEM images of the fabricated ZPC and Cu-BGn incorporated ZPC (Cu-ZPC) to observe the Cu-BGn distribution. (B) XRD results. The circles denote the peaks that appeared similarly in Cu-ZPC (above) and ZPC (below) and closely matched the pattern of ZnO (•). (C) Film thickness for different concentrations (1.5~3.5 wt%) of Cu-BGn incorporated ZPC. Considering the ISO requirements (film thickness ≤ 25 μm), we selected ZPC as the control and Cu-ZPC-2.5 (Cu-ZPC) as the experimental group (n = 5, $p < 0.05$). (D) Compressive strength and (E) compressive modulus showed no significant difference (n = 10, $p > 0.05$), and both satisfied ISO requirements. (F) Micro-Vickers hardness (HV) shows no significance (n = 7, $p > 0.05$), and (G) the arithmetic mean roughness (R_a) result show 'NS' among ZPC and Cu-ZPC (n = 4, $p > 0.05$).

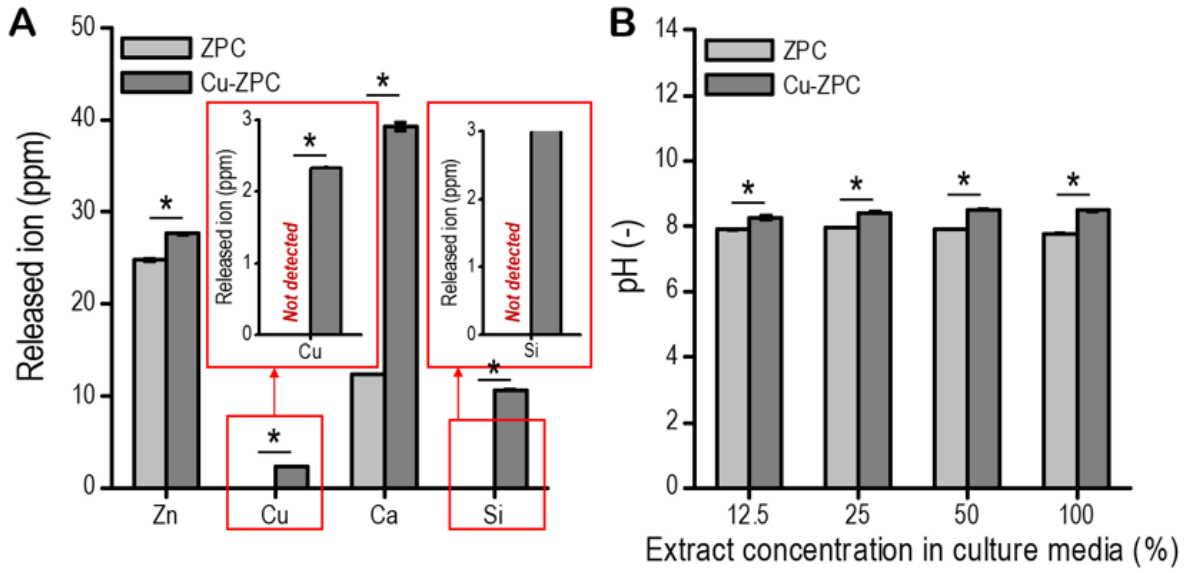

Fig. 3. The ion release of ZPC and Cu-ZPC. (A) The different elemental ion compositions (Zn, Cu, Ca and Si ions) in 100% ZPC (Zn: 24.77 ± 0.15 ppm, Cu: Not detected, Ca: 12.31 ± 0.06 ppm, Si: Not detected) and Cu-ZPC (Zn: 27.68 ± 0.11 ppm, Cu: 2.33 ± 0.01 ppm, Ca: 39.33 ± 0.43 ppm, Si: 10.64 ± 0.09 ppm) using inductively coupled plasma atomic emission spectroscopy. The Cu and Si were presented only in Cu-ZPC, and the percentages of Ca was also relatively higher in Cu-ZPC compared to ZPC. (B) pH measurement in different extract concentration in culture media (12.5~100%) for ZPC (12.5%: 7.92 ± 0.03, 25%: 7.97 ± 0.01, 50%: 7.93 ± 0.02, 100%: 7.77 ± 0.03) and Cu-ZPC (12.5%: 8.27 ± 0.06, 25%: 8.43 ± 0.02, 50%: 8.51 ± 0.01, 100%: 8.47 ± 0.01). Cu-ZPC extracts showed slightly higher pH levels compared to ZPC extracts (n = 3, $p < 0.05$ (*)).

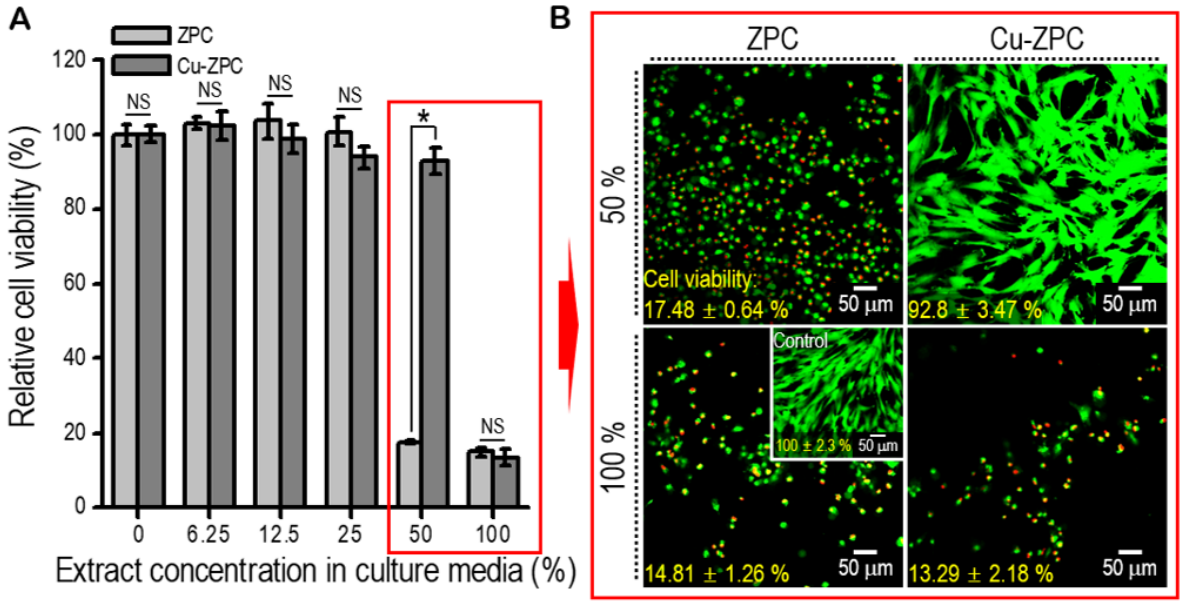

Fig. 4. Summary of the cytotoxicity test. (A) Relative cell viability results based on the MTS assay for different extract concentrations in culture media (0, 6.25, 12.5, 25, 50, and 100%), including (B) live (green)/dead (red) images. All concentrations up to 25% showed high cell viability, but in the case of the 50% extract, Cu-ZPC showed relatively higher cell viability than ZPC due to Cu-BGn (n = 5, $p < 0.05$ (*), $p > 0.05$ ('NS')).

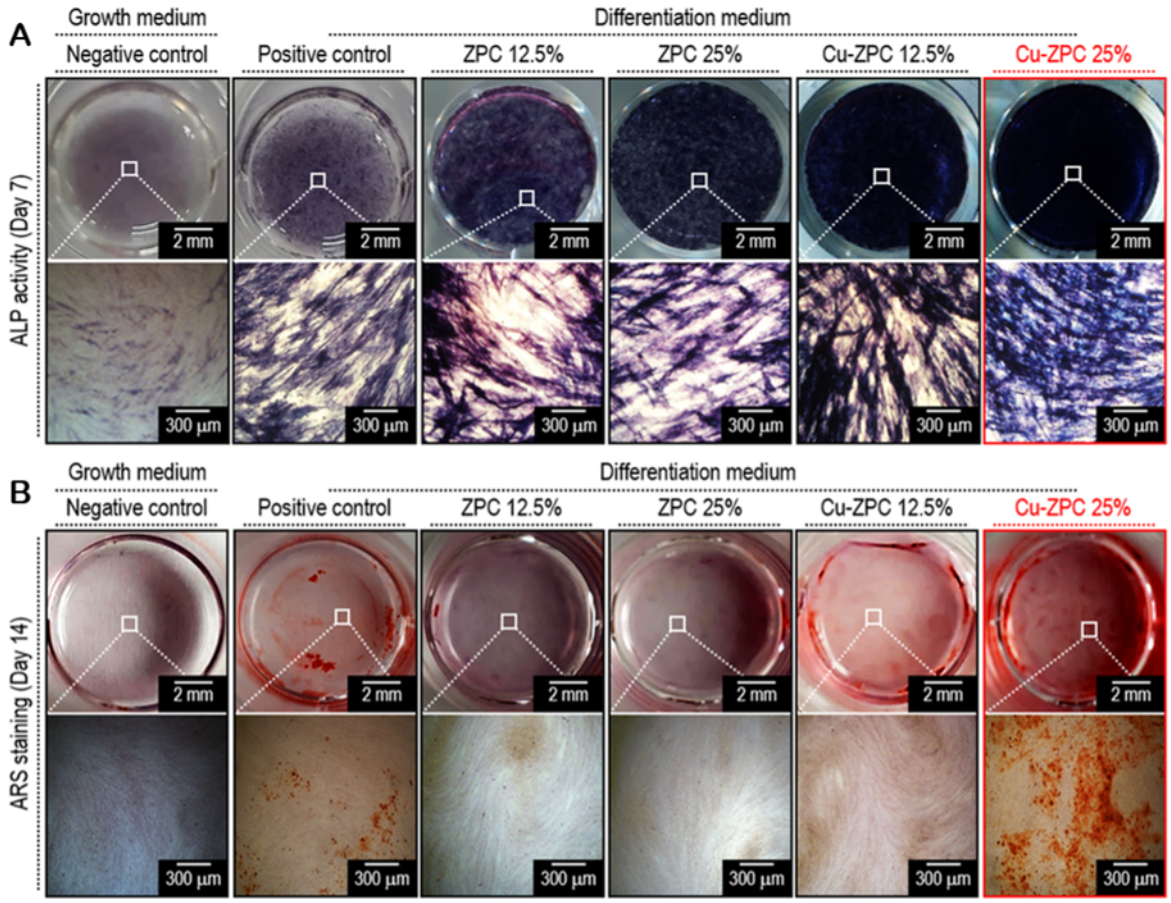

Fig. 5. Odontoblastic differentiation of dental pulp human cells. Optical images from (A) alkaline phosphatase (ALP) activity on Day 7 and (B) alizarin red S (ARS) staining on Day 14 for different extract concentrations (0, 12.5, and 25%) of ZPC and Cu-ZPC. As the controls, negative (dental human pulp cells cultured in growth medium) and positive (dental human pulp cells cultured in differentiation medium) controls were used. Odontoblastic differentiation occurred actively in Cu-ZPC 25%, displaying significant dark blue for ALP and more red colors for ARS staining using dental pulp human cells compared to those of other groups (n = 3).

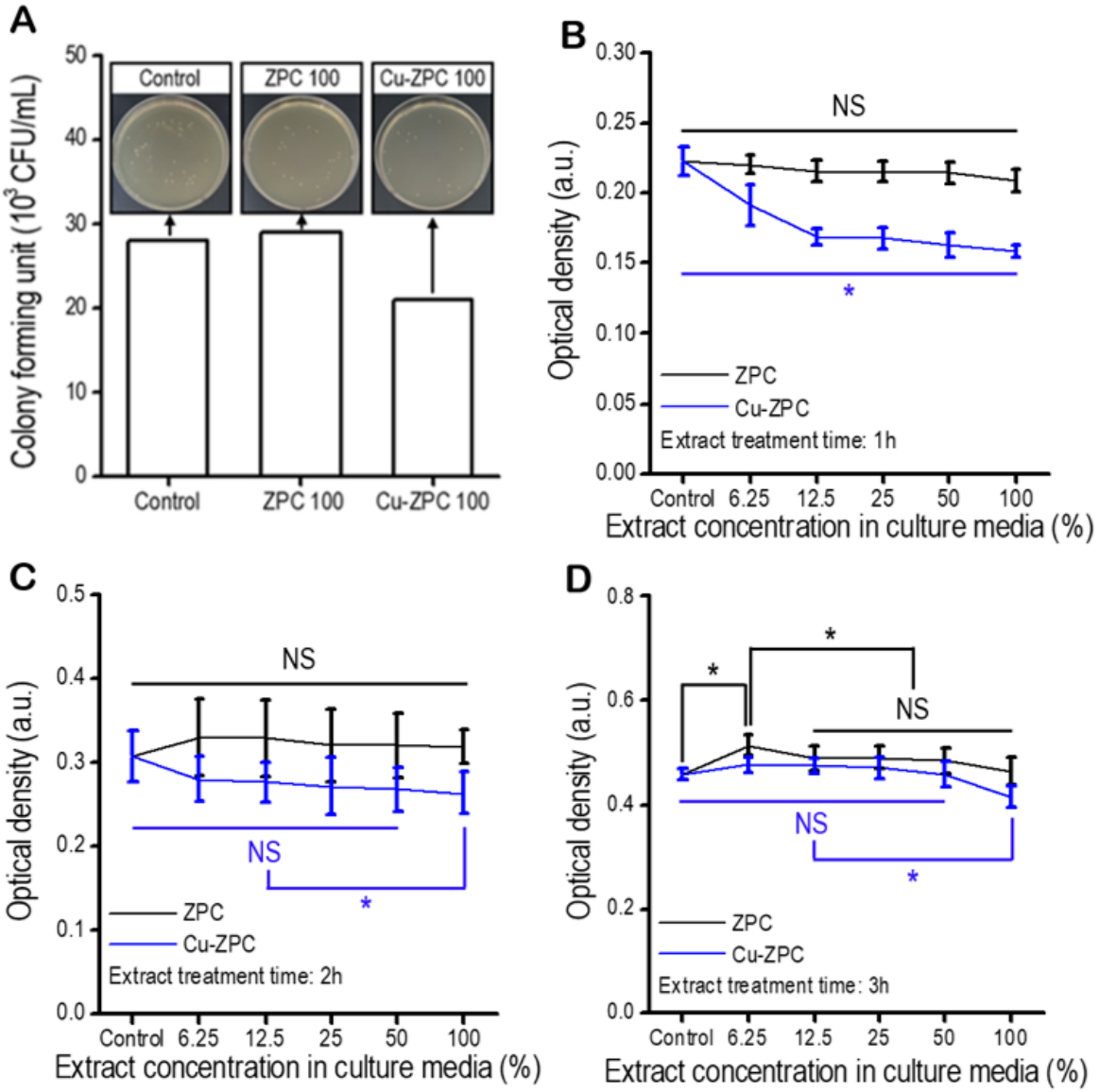

Fig. 6. Antibacterial effects on ZPC and Cu-ZPC extracts. (A) *E. faecalis* concentration on control, ZPC 100%, and Cu-ZPC 100%, including the optical images. (B-D) Optical density results of ZPC and Cu-ZPC extracts (6.25~100%) by adding PrestoBlue compared to the control (no extract group) with different extract treatment times (1~3 h) (n = 8, $p < 0.05$). All analysis were performed at least three times and the representative data and images were added. The Cu-BGn incorporated ZPC extracts showed relatively lower colony forming units (CFUs), indicating significant antibacterial activity compared to the control, however, ZPC extracts showed non-significant ($p > 0.05$ ('NS')) up to different extract treatment times (1~3 h).

▪ References

[1] Anusavice KJ, Shen C, Rawls HR. Phillips' Science of Dental Materials. 12th Editi. 2013.

[2] de Souza Costa CA, Teixeira HM, do Nascimento ABL, Hebling J. Biocompatibility of Resin-Based Dental Materials Applied as Liners in Deep Cavities Prepared in Human Teeth. J Biomed Mater Res 2007;81:175–84.

[3] Lad PP, Kamath M, Tarale K, Kusugal PB. Practical clinical considerations of luting cements: A review. J Int Oral Heal 2014;6:116–20.

[4] Lee JH, Lee HH, Kim KN, Kim KM. Cytotoxicity and anti-inflammatory effects of zinc ions and eugenol during setting of ZOE in immortalized human oral keratinocytes grown as three-dimensional spheroids. Dent Mater 2016;32:e93–104.

[5] Lee JH, Lee HH, Kim HW, Yu JW, Kim KN, Kim KM. Immunomodulatory/anti-inflammatory effect of ZOE-based dental materials. Dent Mater 2017;33:e1–12.

[6] Haddad MF, Rocha EP, Assunção WG. Cementation of Prosthetic Restorations: From Conventional Cementation to Dental Bonding Concept. J Craniofac Surg 2011;22:952–8.

[7] McKenzie MA, Linden RWA, Nicholson JW. The physical properties of conventional and resin-modified glass-ionomer dental cements stored in saliva, proprietary acidic beverages, saline and water. Biomaterials 2003;24:4063–9.

[8] Wetzel R, Eckardt O, Biehl P, Brauer DS, Schacher FH. Effect of poly(acrylic acid) architecture on setting and mechanical properties of glass ionomer cements. Dent Mater 2020;36:377–86.

[9] Fleming GJP, Farooq AA, Barralet JE. Influence of powder/liquid mixing ratio on the performance of a restorative glass-ionomer dental cement. Biomaterials 2003;24:4173–9.

[10] Bagheri R. Film thickness and flow properties of resin-based cements at different temperatures. J Dent 2013;14:57–63.

[11] Waggoner WF, Nelson T. 22-Restorative Dentistry for the Primary Dentition. Sixth Edit. Elsevier Inc.; 2019.

[12] Hübel S, Mejàre I. Conventional versus resin-modified glass-ionomer cement for Class II restorations in primary molars. A 3-year clinical study. Int J Paediatr Dent 2003;13:2–8.

[13] Croll TP, Bar-Zion Y, Segura A, Donly KJ. Clinical performance of resin-modified glass ionomer cement restorations in primary teeth: A retrospective evaluation. J Am Dent Assoc

2001;132:1110–6.

[14] Kim DA, Lee JH, Jun SK, Kim HW, Eltohamy M, Lee HH. Sol–gel-derived bioactive glass nanoparticle-incorporated glass ionomer cement with or without chitosan for enhanced mechanical and biomineralization properties. Dent Mater 2017;33:805–17.

[15] Jung C, Kim S, Sun T, Cho YB, Song M. Pulp-dentin regeneration: current approaches and challenges. J Tissue Eng 2019;10:1–13.

[16] Attar N, Tam L, McComb D. Mechanical and physical properties of contemporary dental luting agents. J Prosthet Dent 2003;89:127–34.

[17] Rosenstiel SF, Land MF, Crispin BJ. Dental luting agents: A review of the current literature. J Prosthet Dent 1998;80:280–301.

[18] Farah JW, Hoodm JAA, Craig RG. Effects of Cement Bases on the Stresses in Amalgam Restorations. J Dent Res 1975;54:10–5.

[19] Wassmann T, Schubert A, Malinski F, Rosentritt M, Krohn S, Techmer K, et al. The antimicrobial and cytotoxic effects of a copper-loaded zinc oxide phosphate cement. Clin Oral Investig 2020;24:3899–909.

[20] Jin GZ, Chakraborty A, Lee JH, Knowles JC, Kim HW. Targeting with nanoparticles for the therapeutic treatment of brain diseases. J Tissue Eng 2020;11:1–13.

[21] Nizami MZI, Takashiba S, Nishina Y. Graphene oxide: A new direction in dentistry. Appl Mater Today 2020;19:100576.

[22] Jo SB, Erdenebileg U, Dashnyam K, Jin GZ, Cha JR, El-Fiqi A, et al. Nano-graphene oxide/polyurethane nanofibers: mechanically flexible and myogenic stimulating matrix for skeletal tissue engineering. J Tissue Eng 2020;11:1–10.

[23] Farooq I, Ali S, Al-saleh S, Alhamdan EM, Alrefeai MH, Abduljabbar T, et al. Synergistic Effect of Bioactive Inorganic Fillers in Enhancing Properties of Dentin Adhesives — A Review. Polymers 2021;13:1–15.

[24] Kim HS, Lee JH, Mandakhbayar N, Jin GZ, Kim SJ, Yoon JY, et al. Therapeutic tissue regenerative nanohybrids self-assembled from bioactive inorganic core / chitosan shell nanounits. Biomaterials 2021;274:120857.

[25] Carvalho SM, Moreira CDF, Oliveira ACX, Oliveira AAR, Lemos EMF, Pereira MM. Chapter

15 - Bioactive glass nanoparticles for periodontal regeneration and applications in dentistry. Elsevier Inc.; 2019.

[26] Zheng K, Dai X, Lu M, Hüser N, Taccardi N, Boccaccini AR. Synthesis of copper-containing bioactive glass nanoparticles using a modified Stöber method for biomedical applications. Colloids Surfaces B Biointerfaces 2017;150:159–67.

[27] Singh RK, Knowles JC, Kim HW. Advances in nanoparticle development for improved therapeutics delivery: nanoscale topographical aspect. J Tissue Eng 2019;10:1–9.

[28] Dashnyam K, El-Fiqi A, Buitrago JO, Perez RA, Knowles JC, Kim HW. A mini review focused on the proangiogenic role of silicate ions released from silicon-containing biomaterials. J Tissue Eng 2017;8:1–13.

[29] Stähli C, James-Bhasin M, Hoppe A, Boccaccini AR, Nazhat SN. Effect of ion release from Cu-doped 45S5 Bioglass® on 3D endothelial cell morphogenesis. Acta Biomater 2015;19:15–22.

[30] Zhao S, Li L, Wang H, Zhang Y, Cheng X, Zhou N, et al. Wound dressings composed of copper-doped borate bioactive glass microfibers stimulate angiogenesis and heal full-thickness skin defects in a rodent model. Biomaterials 2015;53:379–91.

[31] Wu C, Zhou Y, Xu M, Han P, Chen L, Chang J, et al. Copper-containing mesoporous bioactive glass scaffolds with multifunctional properties of angiogenesis capacity, osteostimulation and antibacterial activity. Biomaterials 2013;34:422–33.

[32] Lee NH, Kang MS, Kim TH, Yoon DS, Mandakhbayar N, Jo SB, et al. Dual actions of osteoclastic-inhibition and osteogenic-stimulation through strontium-releasing bioactive nanoscale cement imply biomaterial-enabled osteoporosis therapy. Biomaterials 2021;276:121025.

[33] Lee JH, Mandakhbayar N, El-Fiqi A, Kim HW. Intracellular co-delivery of Sr ion and phenamil drug through mesoporous bioglass nanocarriers synergizes BMP signaling and tissue mineralization. Acta Biomater 2017;60:93–108.

[34] Jun SK, Yang SA, Kim YJ, El-Fiqi A, Mandakhbayar N, Kim DS, et al. Multi-functional nano-adhesive releasing therapeutic ions for MMP-deactivation and remineralization. Sci Rep 2018;8:1–10.

[35] El-Fiqi A, Mandakhbayar N, Jo SB, Knowles JC, Lee JH, Kim HW. Nanotherapeutics for regeneration of degenerated tissue infected by bacteria through the multiple delivery of bioactive

ions and growth factor with antibacterial/angiogenic and osteogenic/odontogenic capacity. Bioact Mater 2021;6:123–36.

[36] Gutiérrez MF, Malaquias P, Matos TP, Szesz A, Souza S, Bermudez J, et al. Mechanical and microbiological properties and drug release modeling of an etch-and-rinse adhesive containing copper nanoparticles. Dent Mater 2017;33:309–20.

[37] Gutiérrez MF, Malaquias P, Hass V, Matos TP, Lourenço L, Reis A, et al. The role of copper nanoparticles in an etch-and-rinse adhesive on antimicrobial activity, mechanical properties and the durability of resin-dentine interfaces. J Dent 2017;61:12–20.

[38] Athanasiadou E, Paschalidou M, Theocharidou A, Kontoudakis N, Arapostathis K, Bakopoulou A. Biological interactions of a calcium silicate based cement (Biodentine™) with Stem Cells from Human Exfoliated Deciduous teeth. Dent Mater 2018;34:1797–813.

[39] Sasaki JI, Kiba W, Abe GL, Katata C, Hashimoto M, Kitagawa H, et al. Fabrication of strontium-releasable inorganic cement by incorporation of bioactive glass. Dent Mater 2019;35:780–8.

[40] Toledano-Osorio M, Aguilera FS, Osorio R, Muñoz-Soto E, Pérez-Álvarez MC, López-López MT, et al. Hydroxyapatite-based cements induce different apatite formation in radicular dentin. Dent Mater 2020;36:167–78.

[41] Bari A, Bloise N, Fiorilli S, Novajra G, Vallet-Regí M, Bruni G, et al. Copper-containing mesoporous bioactive glass nanoparticles as multifunctional agent for bone regeneration. Acta Biomater 2017;55:493–504.

[42] El-Fiqi A, Kim TH, Kim M, Eltohamy M, Won JE, Lee EJ, et al. Capacity of mesoporous bioactive glass nanoparticles to deliver therapeutic molecules. Nanoscale 2012;4:7475–88.

[43] El-Fiqi A, Kim JH, Kim HW. Osteoinductive Fibrous Scaffolds of Biopolymer/Mesoporous Bioactive Glass Nanocarriers with Excellent Bioactivity and Long-Term Delivery of Osteogenic Drug. ACS Appl Mater Interfaces 2015;7:1140–52.

[44] Amornpitoksuk P, Suwanboon S, Sangkanu S, Sukhoom A, Wudtipan J, Srijan K, et al. Synthesis, photocatalytic and antibacterial activities of ZnO particles modified by diblock copolymer. Powder Technol 2011;212:432–8.

[45] Kleverlaan CJ, van Duinen RNB, Feilzer AJ. Mechanical properties of glass ionomer cements affected by curing methods. Dent Mater 2004;20:45–50.

[46] Formosa LM, Mallia B, Camilleri J. The effect of curing conditions on the physical properties

of tricalcium silicate cement for use as a dental biomaterial. Int Endod J 2012;45:326–36.

[47] Hidalgo J, Baghernejad D, Falk A, Larsson C. The influence of two different cements on remaining cement excess in cement-retained implant-supported zirconia crowns. An in vitro study. BDJ Open 2021;7:1–6.

[48] Wang L, D'Alpino PHP, Lopes LG, Pereira JC. Mechanical properties of dental restorative materials: relative contribution of laboratory tests. J Appl Oral Sci 2003;11:162–7.

[49] Dejak B, Młotkowski A, Romanowicz M. Finite element analysis of stresses in molars during clenching and mastication. J Prosthet Dent 2003;90:591–7.

[50] Fleming GJP, Jandu HS, Nolan L, Shaini FJ. The influence of alumina abrasion and cement lute on the strength of a porcelain laminate veneering material. J Dent 2004;32:67–74.

[51] Zhao J, Xie D. Effect of nanoparticles on wear resistance and surface hardness of a dental glass-ionomer cement. J Compos Mater 2009;43:2739–52.

[52] Behr M, Rosentritt M, Loher H, Kolbeck C, Trempler C, Stemplinger B, et al. Changes of cement properties caused by mixing errors: The therapeutic range of different cement types. Dent Mater 2008;24:1187–93.

[53] Gharechahi M, Moosavi H, Forghani M. Effect of Surface Roughness and Materials Composition on Biofilm Formation. J Biomater Nanobiotechnol 2012;3:541–6.

[54] Brajkovic D, Antonijevic D, Milovanovic P, Kisic D, Zelic K, Djuric M, et al. Surface characterization of the cement for retention of implant supported dental prostheses: In vitro evaluation of cement roughness and surface free energy. Appl Surf Sci 2014;311:131–8.

[55] Kang MS, Lee NH, Singh RK, Mandakhbayar N, Perez RA, Lee JH, et al. Nanocements produced from mesoporous bioactive glass nanoparticles. Biomaterials 2018;162:183–99.

[56] Seo JJ, Mandakhbayar N, Kang MS, Yoon JY, Lee NH, Ahn J, et al. Antibacterial, proangiogenic, and osteopromotive nanoglass paste coordinates regenerative process following bacterial infection in hard tissue. Biomaterials 2021;268:120593.

[57] Jun SK, Lee JH, Lee HH. The Biomineralization of a Bioactive Glass-Incorporated Light-Curable Pulp Capping Material Using Human Dental Pulp Stem Cells. Biomed Res Int 2017;2017:1–9.

[58] Lee JH, Seo SJ, Kim HW. Bioactive glass-based nanocomposites for personalized dental tissue

regeneration. Dent Mater J 2016;35:710–20.

[59] Michot B, Casey SM, Gibbs JL. Effects of Calcitonin Gene-related Peptide on Dental Pulp Stem Cell Viability, Proliferation, and Differentiation. J Endod 2020;46:950–6.

[60] Im GB, Lee J, Song J, Yu T, Bhang SH. Novel angiogenic metal nanoparticles controlling intracellular gene activation in stem cells. Chem Eng J 2021;419:129487.

[61] Li W, Mao M, Hu N, Wang J, Huang J, Zhang W, et al. A graphene oxide-copper nanocomposite for the regeneration of the dentin-pulp complex: An odontogenic and neurovascularization-inducing material. Chem Eng J 2021;417:129299.

[62] Westhauser F, Wilkesmann S, Nawaz Q, Hohenbild F, Rehder F, Saur M, et al. Effect of manganese, zinc, and copper on the biological and osteogenic properties of mesoporous bioactive glass nanoparticles. J Biomed Mater Res - Part A 2021;109:1457–67.

[63] Lewinstein I, Matalon S, Slutzkey S, Weiss EI. Antibacterial properties of aged dental cements evaluated by direct-contact and agar diffusion tests. J Prosthet Dent 2005;93:364–71.

[64] Mayanagi G, Igarashi K, Washio J, Nakajo K, Domon-Tawaraya H, Takahashi N. Evaluation of pH at the bacteria-dental cement interface. J Dent Res 2011;90:1446–50.

[65] Imazato S, Kohno T, Tsuboi R, Thongthai P, Xu HHK, Kitagawa H. Cutting-edge filler technologies to release bio-active components for restorative and preventive dentistry. Dent Mater J 2020;39:69–79.

[66] Kohno T, Liu Y, Tsuboi R, Kitagawa H, Imazato S. Evaluation of ion release and the recharge ability of glass-ionomer cement containing BioUnion filler using an in vitro saliva-drop setting assembly. Dent Mater 2021;37:882–93.